Generation of 17q21.31 duplication iPSC-derived neurons as a model for primary tauopathies

Laetitia Miguel, Anne Rovelet-Lecrux, Pascal Chambon, Géraldine Joly-Helas, Stéphane Rousseau, David Wallon, Stéphane Epelbaum, Thierry Frébourg, Dominique Campion, Gaël Nicolas, et al.

Stem Cell Research 61 (2022) 102762

Contents lists available at ScienceDirect

Stem Cell Research

journal homepage: www.elsevier.com/locate/scr

Generation of 17q21.31 duplication iPSC-derived neurons as a model for primary tauopathies

Laetitia Miguel [a], Anne Rovelet-Lecrux [a], Pascal Chambon [a], Géraldine Joly-Helas [a], Stéphane Rousseau [a], David Wallon [b], Stéphane Epelbaum [c], Thierry Frébourg [a], Dominique Campion [a], Gaël Nicolas [a], Magalie Lecourtois [a,*]

[a] Normandie Univ, UNIROUEN, Inserm U1245, CHU Rouen, Department of Genetics and CNR-MAJ, FHU G4 Génomique, F-76000 Rouen, France
[b] Normandie Univ, UNIROUEN, Inserm U1245, CHU Rouen, Department of Neurology and CNR-MAJ, FHU G4 Génomique, F-76000 Rouen, France
[c] AP-HP, Groupe Hospitalier Pitié-Salpètrière, Département de Neurologie, Institut de la mémoire et de la maladie d'Alzheimer, Groupe Hospitalier Pitié-Salpètrière, ICM, CNRS UMR 7225, Inserm U 1127, UPMC-P6 UMR S 1127, GH Pitié-Salpètrière, Paris, France

ARTICLE INFO

Keywords:
Tauopathies
iPSC-induced neurons
MAPT
17q21.31
Tau

ABSTRACT

Tau proteins belong to the microtubule associated protein family and are mainly expressed in neurons. Tau accumulates in patients' brain in several neurodegenerative diseases, including Fronto-temporal dementia and Alzheimer's disease. Recently, we described a 17q21.31 duplication in patients presenting different cognitive or motor symptoms and characterized by the accumulation of different Tau isoforms. This duplication involves four genes, including the *MAPT* gene that encodes the Tau protein. The main pathophysiological consequence associated with this duplication was a 1.6–1.9-fold increase in the *MAPT* messenger RNA as measured in blood samples of duplication carriers. However, the pathophysiological consequences of this duplication in a cell type relevant for neurodegenerative diseases have never been explored so far. In this study, we developed the first model of primary tauopathy linked to a 17q21.31 duplication in iPSC-induced neurons from 2 unrelated carriers. As in patients' blood, we demonstrated that this duplication was associated with an increase in *MAPT* mRNA resulting in elevated Tau protein levels in iPSC-derived cortical neurons. We believe that these iPSC lines will be a pertinent tool to elucidate how a same genetic cause could lead to distinct types of tauopathies and the pathophysiological mechanisms associated with Tau-mediated neurodegeneration in the 17q21.31 duplication context.

1. Introduction

Tau is a protein predominantly expressed in the central and peripheral nervous system, where it is most abundant in nerve cell axons. Tau proteins are encoded by the *MAPT* gene located on the long arm of chromosome 17 (17q21) that generates a total of 6 Tau protein isoforms through alternative splicing of exons 2, 3, and 10 (Goedert et al., 1989). Regulated expression of exons 2 and 3 gives rise to Tau isoforms with 0, 1, or 2 N-terminal inserts, whereas exclusion or inclusion of exon 10 leads to expression of Tau isoforms with three (3R) or four (4R) microtubule-binding domains (Caillet-Boudin et al., 2015; Himmler et al., 1989). Apart from being a stabilizer of microtubules and being involved in their dynamics, Tau plays a role in several physiological processes including myelination, axonal transport, neurogenesis, motor function, learning and memory, neuronal excitability, glucose metabolism, iron homeostasis, and DNA protection (Kent et al., 2020).

Under pathological conditions, aberrant assembly of highly phosphorylated Tau into insoluble aggregates is observed in neurons and glial cells in a wide range of neurodegenerative disorders, collectively referred to as tauopathies (Ferrer et al., 2014; Wang and Mandelkow, 2016). These diseases are classified as primary tauopathies (e.g., Pick's disease (PiD), corticobasal degeneration (CBD), progressive supranuclear palsy (PSP), FTDP-17), when Tau is the driving pathological factor, or secondary tauopathies (e.g., Alzheimer's Disease (AD)), when Tau is associated with other neuropathological features, namely the Aβ peptide in AD. Furthermore, depending on the pathology, the distribution, aspect and composition of Tau aggregates are distinct. As a consequence, tauopathies can be subdivided into 3R, 4R or mixed 3R/4R subtypes according to the respective predominance of Tau isoforms found in brain aggregates (Kovacs, 2017; Mailliot et al., 1998; Sergeant

* Corresponding author.
E-mail address: magalie.lecourtois@univ-rouen.fr (M. Lecourtois).

https://doi.org/10.1016/j.scr.2022.102762
Received 2 August 2021; Received in revised form 7 March 2022; Accepted 21 March 2022
Available online 22 March 2022

et al., 1999). For instance, PSP and CBD exhibit accumulation of 4R isoforms, both 3R and 4R accumulate in AD, whereas in PiD, 3R isoforms are the main constituent of the aggregates (Irwin, 2016). In addition, corresponding aggregates are enriched in distinct brain regions (e.g. cortex versus basal ganglia) and cell types (neurons, astrocytes) depending on the primary disorder. *MAPT* point mutations have been identified in patients with a primary tauopathy, but the genetic causes remain unexplained in most patients.

Duplications of the 17q21.31 chromosomal region were identified in patients clinically diagnosed with distinct phenotypes, from severe memory impairment with or without behavioral changes (Chen et al., 2019; Hooli et al., 2014; Le Guennec et al., 2017; Rovelet-Lecrux et al., 2010), to atypical extrapyramidal syndromes (Chen et al., 2019). The 17q21.31 duplication is a rare recurrent 439 kb-long structural variant encompassing 4 genes, *MAPT, KANSL1, CRHR1*, and *STH* (Chen et al., 2019; Hooli et al., 2014; Le Guennec et al., 2017; Rovelet-Lecrux et al., 2010). To decipher the phenotypic spectrum associated with the 17q21.31 duplication, we recently studied ten 17q21.31 duplication carriers gathering clinical, biological, imaging and neuropathological data (Wallon et al., 2021). Neuropathological examination exclusively showed Tau deposits. Distribution, aspect and composition of the 4R/3R Tau aggregates revealed a spectrum ranging from predominantly 3R, mainly cortical deposits well correlating with cognitive and behavioral changes, to predominantly 4R deposits, mainly in the basal ganglia and midbrain, in patients with prominent extrapyramidal syndrome. Altogether, these studies suggest that 17q21.31 duplication causes a primary tauopathy associated with diverse clinical and neuropathological features. The main pathophysiological consequence associated with this duplication so far is a 1.6–1.9 fold increase in the *MAPT* messenger RNA as measured in blood samples of duplication carriers (Le Guennec et al., 2017). Hence, the pathophysiological consequences of the 17q21.31 duplication in a cell type relevant for neurodegenerative diseases remain to be explored.

Functional studies are generally limited by the lack of reliable *in vitro* models of human neurons. Patient-derived induced pluripotent stem cells (iPSCs) have emerged as a powerful resource to study the molecular mechanisms underlying neurodegenerative diseases. Importantly, patient's somatic cell reprogramming offers the opportunity to study the effect of complex genomic rearrangements such as copy number variations, which are difficult to recreate in a dish with genome editing tools while preserving the patient genetic context. The iPSCs can be differentiated into multiple cell types, including neuronal and glial subtypes affected in primary tauopathies, enabling the study of Tau biology in a human cellular model that may more faithfully reflect the endogenous condition.

In this study, we describe the first 17q21.31 duplication iPSC-derived neuron model. We generated iPSC lines from fibroblasts of 2 patients with primary tauopathy carrying the 17q21.31 duplication and 2 healthy controls. The developed iPSC lines attained pluripotency characteristics and were able to differentiate towards the neuronal fate. In this model, the 17q21.31 duplication lead to an increase in *MAPT* mRNA expression levels, resulting in an increase in Tau protein steady-state levels in iPSC-derived neurons. We believe that these iPSC lines could be a pertinent tool to study the pathophysiological consequences of Tau accumulation, independently of *MAPT* mutations, while overcoming exogenous overexpression techniques.

2. Material and methods

2.1. Patients and fibroblast reprogramming

Skin biopsies of 2 patients (ALZ-596-001 named DUP-1 and ROU-1373-001 named DUP-2) and 2 controls (ALZ-596-005 named CTRL-1, DUP-1's brother and ROU-1333-002 named CTRL-2) were performed following a written informed consent from donors or legal representatives. This study was approved by the CPP Ile de France II ethics committee. Phenotypic characteristics of the 17q21.31 duplication carriers were previously described in (Le Guennec et al., 2017) and more recently in (Wallon et al., 2021). Fibroblasts from skin biopsies were isolated and grown at the Laboratory of Cytogenetics of the Rouen University Hospital, France. Reprogramming of fibroblasts into iPSCs was realized by transduction with non-integrating Sendai virus carrying *OCT3/4*, *SOX2*, *KLF4* and *cMYC* (Thermo Fischer Scientific Inc., Waltham, MA) by the iPSC Core facility of Nantes, France. Briefly, cells showing morphological evidence of reprogramming were selected manually and clonally expanded. The resulting clones were analyzed for pluripotency markers by quantitative PCR and absence of Sendai virus integration into the genome. Chromosomal abnormalities were investigated by karyotyping. Two over three clones from patient DUP-1 carried chromosomal rearrangements and were consequently excluded from the study.

2.2. iPSC culture

Human iPSCs were cultured on feeder-free conditions in mTeSR Plus medium (STEMCELL Technologies, Vancouver, Canada) on Matrigel-coated culture dishes (Corning, Corning, NY, diluted in DMEM-F12 according to manufacturer's instructions). Cells were maintained at 37 °C/5% CO_2 and were split as necessary based on colony growth (5–6 days) using StemMACS XF passaging solution (Miltenyi Biotec). Differentiating colonies were removed from the plate before splitting. Cell lines were confirmed to be free of mycoplasma.

2.3. Neural induction and cortical neuron differentiation

Human iPSCs were differentiated into cortical neurons according to (Shi et al., 2012). Briefly, neural induction was performed when cells reached 100% confluency by switching them to neural induction medium (DMEM/F12 - Neurobasal 1:1 supplemented with B27 and N2 (Thermo Fischer Scientific Inc.), 1 μM LDN-193189 (Sigma Aldrich, St-Louis, MO) and 10 μM SB431542 (Tocris Biosciences, Bristol, UK). Medium was changed every day during 8 days, achieving a characteristic neuroepithelial cell morphology by day 8. The neuroepithelial sheet was dissociated using 1u/mL dispase (STEMCELL Technologies) and plated on Matrigel-coated culture dishes. Neural Stem Cells (NSCs) were maintained in proliferative state in neural expansion medium (DMEM/F12 - Neurobasal 1:1 supplemented with B27 and N2 containing 10 ng/mL FGF-2 and EGF-1 (Cell guidance Systems Ltd., Cambridge, UK). When substantial neurogenesis occurred, NSCs were passaged using StemPro Accutase (Thermo Fischer Scientific Inc.) to obtain single cells. NSCs were plated at 200,000 NSCs/cm^2 into Matrigel-coated culture dishes and on the following day, cells were differentiated in cortical neurons by FGF-2/EGF-1 withdrawal concomitantly with gamma-secretase inhibition (10 nM compound E, Abcam, Cambridge, UK) for 12 days. From this point, the cell culture medium was shifted gradually to Brainphys™ medium with N2-A and SM1 supplements (STEMCELL Technologies) and complemented with 10 ng/mL BDNF and GDNF (Cell Guidance Systems Ltd.), 10 nM Trichostatin A (Abcam) and 1 μM cAMP (Sigma Aldrich). Medium was changed every other day for 12 days. Half medium change was then realized twice a week until the specified maturation time.

2.4. RNA extraction and RT-PCR/qPCR

Cells were dissociated using trypsin-EDTA (Thermo Fischer Scientific Inc.), centrifuged 3 min at 3,000×*g* and rinsed twice in cold PBS. iPSC and NSC pellets were extracted using Nucleospin RNA kit and neurons using Nucleospin RNA XS kit (Macherey-Nagel GmbH and Co. KG, Düren, Germany). Five hundred ng of total RNA was reverse-transcribed into cDNA, using the RETROscript Reverse Transcription kit (Thermo Fisher Scientific Inc.) with Oligo(dT) primers according to the manufacturer's instructions for 2-Step RT-PCR without heat denaturation.

PCR reaction were realized as previously described (Miguel et al., 2019) (Supplementary Table 2). qPCR reactions were performed in a final volume of 20 μL, using the SsoFast Evagreen Supermix (Bio-Rad Laboratories, Hercules, CA) with primers at a final concentration of 250 nM (Supplementary Table 2). PCR amplifications were performed on a CFX96 Real-Time System thermal cycler (Bio-Rad Laboratories) using the following cycling steps: enzyme activation at 98 °C for 2 min; denaturation and annealing/extension, respectively, at 98 °C for 10 s and 60 °C for 15 s (40 cycles). The comparative -ΔΔCt method was used to determine quantitative values for gene expression levels in each sample using *MAP2* as housekeeping gene.

2.5. Protein extraction and immunoblot analysis

Cells were homogenized in Pierce® RIPA buffer (Thermo Fisher Scientific Inc.), supplemented with a cocktail of protease inhibitors (Sigma-Aldrich). After 30 min on ice, and centrifugation (11,300×*g*, 20 min, 4 °C), the supernatant containing soluble proteins was collected. Proteins were resolved on a 10% SDS-PAGE, transferred onto nitrocellulose membranes using the Trans-Blot Turbo system (Bio-Rad Laboratories) and blocked with 5% non-fat milk. The following antibodies were used in this study: Polyclonal Rabbit Anti-Human Tau (Dako Denmark A/S, Glostrup, Denmark) (1:50,000) and Monoclonal Mouse Neuron-specific beta-III Tubulin (TUBB3) Antibody (TUJ-1 clone; R&D Systems, Inc., Minneapolis, MN) (1:1000). Membranes were incubated with peroxidase-labelled anti-mouse or anti-rabbit antibodies (1:10,000) (Jackson Immunoresearch Laboratories, West Grove, PA), and signals were detected using chemiluminescence reagents (ECL Clarity, Bio-Rad Laboratories). Signals were acquired with a GBOX (Syngene, Cambridge, UK) monitored by the Gene Snap (Syngene) software.

2.6. Immunohistochemistry

Cells were fixed in PBS containing 4% paraformaldehyde for 15 min at room temperature, permeabilized for 15 min in PBS-0.1% Triton X-100 and blocked for one hour in PBS-0.1% Triton X-100–0.5% BSA. Next, cells were incubated with primary antibodies for 1 h at room temperature. We used the following primary antibodies: Monoclonal Mouse anti-Nestin (1:300; Abcam), Polyclonal Rabbit anti-PAX6 (1:300; Biolegend, San Diego, CA), Monoclonal Mouse anti-synaptophysin (H-8 clone; 1:300; Santa Cruz Biotechnology, Inc., Dallas, TX), Monoclonal Mouse TUBB3 Antibody (TUJ-1 clone; 1:1,000; R&D Systems, Inc.), Polyclonal Rabbit Anti-Human Tau (Dako Denmark A/S; 1:1,000) and Polyclonal Rabbit Anti-Human MAP-2 Antibody (H-300 clone; 1:500; Santa Cruz Biotechnology). After three PBS washes, cells were labelled with fluorescent-conjugated antibodies diluted to 1:300 (Molecular probes, Eugene, OR) for 1 h at room temperature. After three PBS washes, nuclei were stained using NucBlue fixed cells ReadyProbes reagent (Molecular probes) according to manufacturer's instructions and coverslips were finally mounted in Prolong diamond (Thermo Fischer Scientific Inc.). Fluorescence images from NSCs were acquired after automatic exposure using an AxioPlan 2 microscope (Zeiss, Iéna, Germany) monitored by the AxioVision software (Zeiss). Fluorescence images from neurons were acquired after automatic exposure using a Leica THUNDER Imaging System (Leica Microsystems, Wetzlar, Germany), combining Computational Clearing with Large Volume adaptative deconvolution (LVCC) for post-acquisition processing.

2.7. Statistical analysis

Statistical analyses were performed using a two-tailed Student's *t*-test with Welch's correction using the GraphPad Prism software (GraphPad, San Diego, CA). All n reported are biological replicates. Statistical significance was defined as ns (not significant) $p > 0.05$, * $p < 0.05$, ** $p < 0.01$, *** $p < 0.001$, **** $p < 0.0001$. All data are presented as mean ± standard error of the mean (SEM).

3. Results and discussion

3.1. Generation and characterization of iPSC lines from healthy individuals and patients carrying a 17q21.31 duplication

Skin punches were obtained from 4 males (Supplementary Table S1), two 17q21.31 duplication carriers and two controls without any cognitive decline nor neurological disease. Skin fibroblasts were reprogrammed into iPSCs by lentiviral transduction with a polycistronic vector encoding the Yamanaka factors (*OCT4*, *KLF4*, *SOX2* and *c-MYC*). iPSCs colonies were then manually picked upon emergence and amplified. Multiple clones were available for each line. Preservation of normal karyotype was confirmed in two clones per individual except for the DUP-1 patient for which only a single clone did not show karyotypic abnormality. The presence of the 17q21.31 duplication in patient's iPSC clones was confirmed by QMPSF (Supplementary Fig. S1). For each clone, pluripotency was verified by expression of pluripotency markers (*POU5F1* and *NANOG)* by RT-PCR (Fig. 1A). To test their ability to differentiate into each of the three germ layers –endoderm, mesoderm, and ectoderm- iPSCs were cultured in defined media and then assayed for expression of markers of the different germ layers by RT-PCR. After the proper differentiation, all clones derived in (i) mesoderm lineage expressed *MSX1*, (ii) endoderm lineage expressed *SOX17* and *FOXA2* and (iii) ectoderm lineage expressed *PAX6* (Supplementary Fig. 2). Note that these markers were never expressed in iPSCs. These results show that all iPSCs clones, from healthy individuals or 17q21.31 duplication carriers, demonstrate pluripotency capability leading to cell types of each of the three germ layers.

3.2. Differentiation of the iPSC lines in cortical neurons

Each iPSC clone was differentiated into NSCs using previously published protocols (Shi et al., 2012). After 8 days, the efficiency of neural induction was monitored by RT-PCR (Fig. 1A) and immunohistochemistry (Fig. 2). All clones displayed a striking down-regulation of the *NANOG* and *POU5F1* pluripotency gene markers compared to iPSCs, indicating the loss of their pluripotency ability (Fig. 1A). Concomitantly, we observed a substantial up-regulation of the NSCs markers *OTX-1* and *FOXG1*, indicating their determination through neuronal fate. Accordingly, newly generated NSCs were immunoreactive for Nestin, an intermediate filament protein expressed in dividing cells during the early stages of development in the central nervous system, and for the neuroepithelial marker PAX6, an essential protein involved in cortical neurogenesis and the formation of cortical layers (Manuel et al., 2015) (Fig. 2). Furthermore, all lines displayed the same ability to generate neuronal rosettes (Fig. 2), the *in vitro* developmental signature of neuroepithelial progenitors (Wilson and Stice, 2006).

Neural progenitors were then differentiated into cortical neurons by feeding them with Brainphys™ medium. After differentiation, cortical gene expression was assessed by RT-PCR using *TBR1*, a deep layer marker of the cerebral cortex, and *Reelin* (*RELN*) that is expressed in later-born neurons of the superficial cortical layer. Both markers were expressed (Fig. 1B), confirming a cortical identity of the neuronal cultures. Furthermore, the iPSC-derived neurons were immunoreactive for the pan-neuronal marker TUBB3 (βIII-tubulin) (Fig. 3A), a common neuronal marker expressed in neurons of both peripheral and central nervous system. As expected in iPSC-derived neurons (García-León et al., 2018; Verheyen et al., 2018), Tau and MAP2 markers, labelling

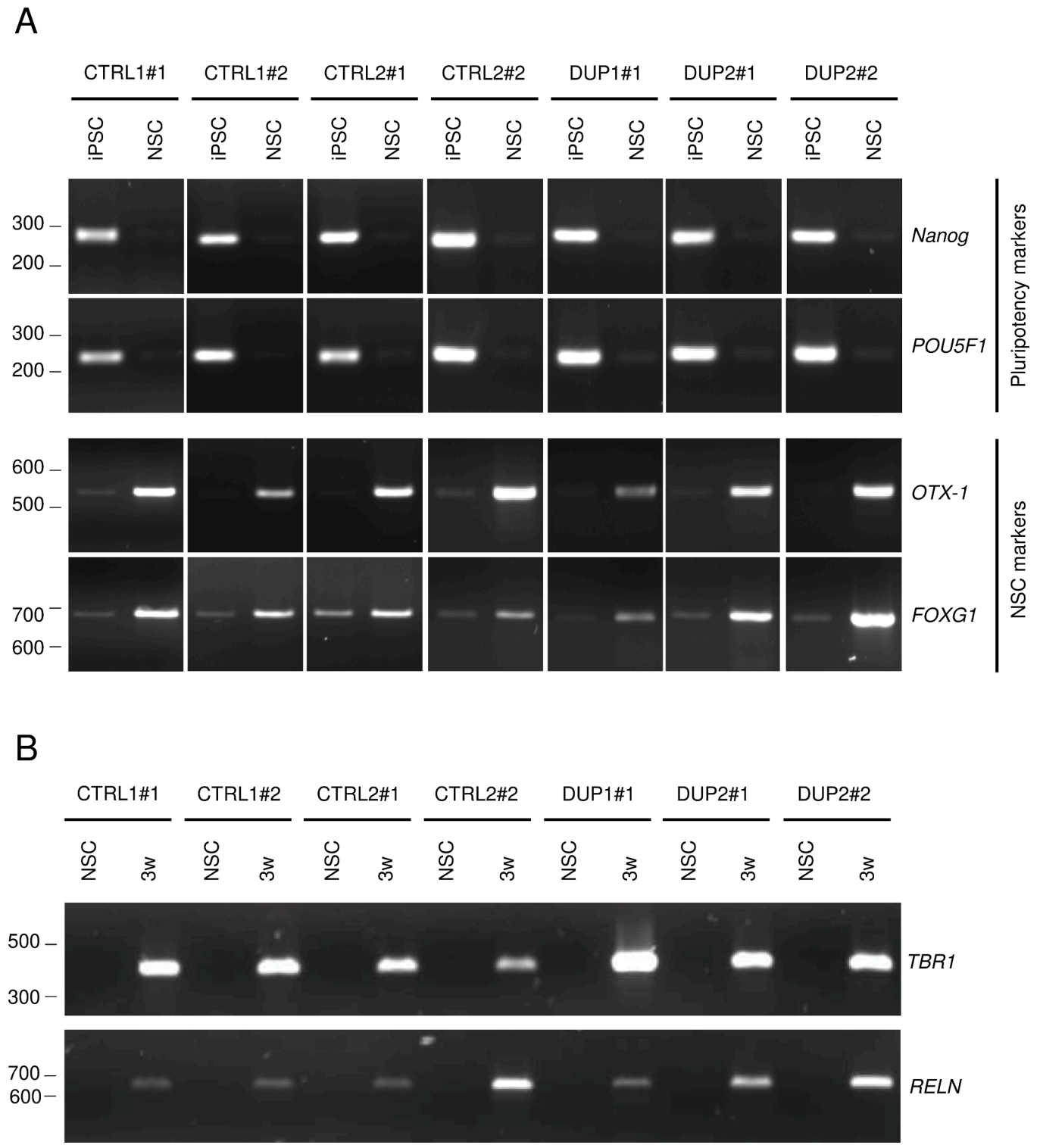

Fig. 1. Expression of pluripotency, NSC and cortical neuron markers in iPSCs, iPSC-induced NSC and iPSC-induced neurons. (A) RT-PCR analyses on mRNA extracted from each clone of iPSCs or iPSC-induced NSCs 7 days post neural induction using *Nanog* and *POU5F1* as pluripotency markers and *OTX-1* and *FOXG1* as NSC markers. *Nanog* and *POU5F1* are both expressed in all iPSC clones and subsequently downregulated 7 days after neural induction (NSC). Conversely, *OTX-1* and *FOXG1* are both upregulated in NSCs, compared to iPSCs. (B) RT-PCR analyses on mRNA extracted from each clone of iPSC-induced NSCs or 3-weeks iPSC-induced neurons using *TBR1* and *RELN* as markers of deep and superficial cortical layer, respectively. Both markers, absent at the NSC stage, are expressed in 3-weeks differentiated neurons. Similar results were obtained in at least 3 independent neural inductions. A representative panel is presented.

axons and dendrites, respectively, were also detected, indicating the achievement of a proper neuronal architecture (Fig. 3A, B). Finally, the pre-synaptic marker synaptophysin (SYP) was located along neurites (Fig. 3B, C). These results indicated that iPSC-induced neurons display neuron-specific morphology and expression of markers reminiscent of *in vivo* neurogenesis and human cortical neurons. No obvious difference was observed between control and patient's lines suggesting that neuronal differentiation capability is not impaired in cells carrying the

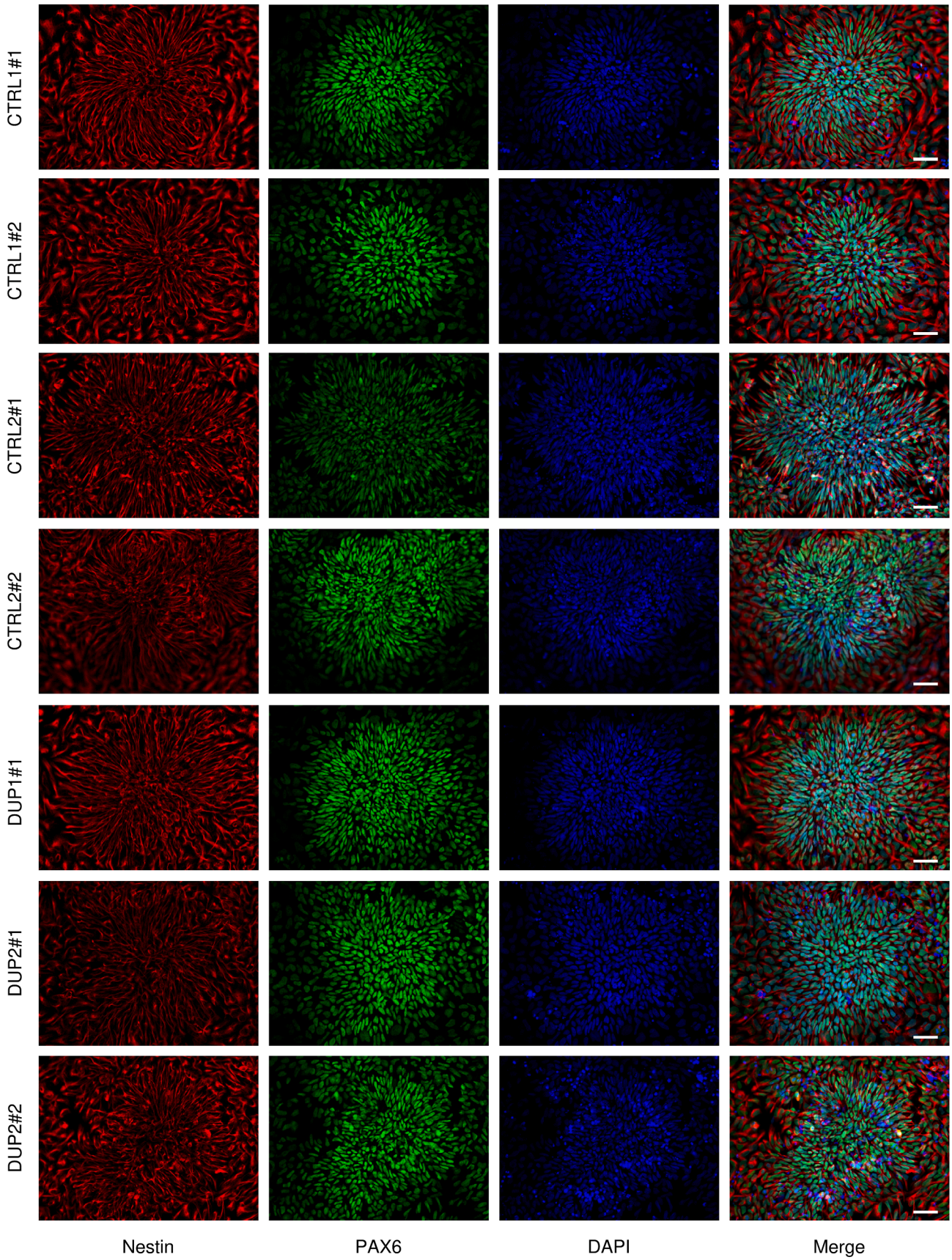

Fig. 2. Immunofluorescence characterization of NSCs. iPSC-induced NSCs were fixed and immunostained 7 days following neural induction using Nestin (Red) and PAX6 antibodies (Green), and counter-stained with DAPI (Blue). Scale bar = 50 μm. (For interpretation of the references to colour in this figure legend, the reader is referred to the web version of this article.)

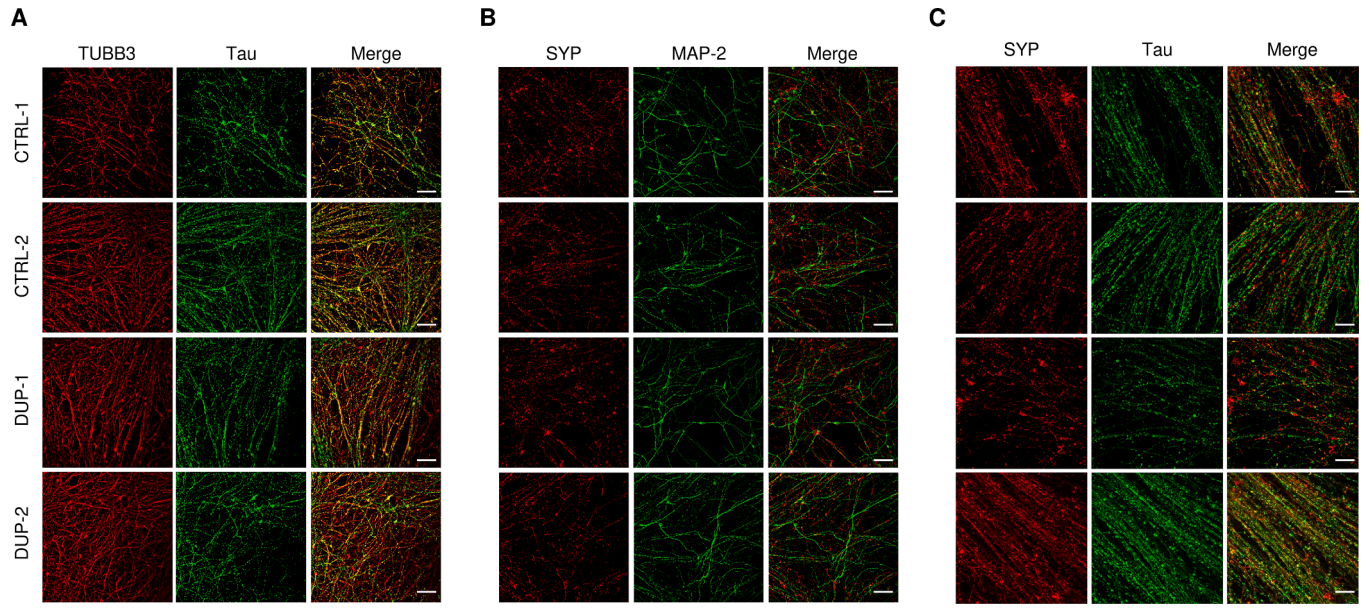

Fig. 3. Immunofluorescence characterization of iPSC-induced neurons. iPSC-induced neurons differentiated for 3 weeks were fixed and immunostained using TUBB3 (Red, A), Tau (Green, A and C), MAP-2 (Green, B), and SYP (Red, B and C) antibodies. Scale bar = 50 μm (A and B) and 20 μm (C). One clone per individual is presented.

17q21.31 duplication.

3.3. Increase in Tau steady-state levels in iPSC-derived neurons carrying a 17q21.31 duplication

We next examined the biological consequences of 17q21.31 duplication on Tau accumulation in iPSC-derived neurons. First, we analyzed total *MAPT* mRNA expression by RT-qPCR using a primer pair targeting all *MAPT* isoforms and *MAP2*, as housekeeping gene. Compared to control (CTRL-1 = 100; CTRL-2 = 107.9), both patients showed a significant increase ($p < 0.0001$) of *MAPT* mRNA relative expression levels (DUP-1 = 213.4; DUP-2 = 171.3) in agreement with a third transcriptionally active copy of the *MAPT* gene (Fig. 4A). To determine if this increase in *MAPT* mRNA expression level in patients was accompanied with an increase in Tau protein steady-state levels, we next performed western blot analyses on protein extracted from control and patient's iPSC-induced neurons using a total Tau antibody. As expected, Tau proteins migrate between 50 and 60 kDa as several bands likely corresponding to different phosphorylation states in control cells (Fig. 4B). The Tau migration profile remained the same in patient's cells. Tau protein quantities were normalized using the pan-neuronal marker TUBB3 (Fig. 4C). Compared to control lines (CTRL-1 = 100; CTRL-2 = 108.7), a significant increase ($p = 0.0004$) of Tau accumulation level was detected in patient's lines (DUP-1 = 268.9; DUP-2 = 180.6). No staining was detected using anti-Tau AT8, MC1 or PHF1 antibodies (Goedert et al., 1995; Greenberg et al., 1992; Jicha et al., 1997) (data not show), suggesting that prolonged culturing might be required to accumulate abnormally phosphorylated Tau species and/or protein with conformational defects.

Interestingly, although not reaching significance, a tendency to an increase in quantities of Tau, both at the mRNA and protein level, is systematically observed in DUP-1 patient in comparison with DUP-2. We have to point out that, because of genomic rearrangements, only one clone was analyzed for DUP-1 patient and it will be essential to confirm this modest increase on an additional clone. A recent study demonstrated that mature dopaminergic iPSC-derived neurons showed haplotype-dependent variations in *MAPT* expression, with the *MAPT* H1 haplotype expressing 22% higher levels of *MAPT* than H2 (Beevers et al., 2017). However, in the present study, DUP-1 patient was carrying 2 copies of the H2 haplotype whereas DUP-2 patient 2 copies of the H1 haplotype (Supplementary Table S1). Therefore, the subtle increase observed in DUP-1 might not be due to the haplotype composition. This disparity in *MAPT* expression between patients carrying the same genomic alteration could be due to other factors, including genetic background or changes in the neuronal subtypes composition inside the culture between clones, individuals or experiments (Volpato and Webber, 2020). Altogether, these results indicate that, in agreement with the data previously obtained from patient's blood, the 17q21.31 duplication causes a rise in *MAPT* expression, resulting in an increase in Tau protein levels in iPSC-induced neurons from two patients.

4. Conclusions

In this study, we developed the first model of primary tauopathy linked to the 17q21.31 duplication in iPSC-induced neurons. As previously shown in patient's blood, we demonstrated that this duplication was associated with a moderate increase in *MAPT* mRNA resulting in elevated Tau protein levels in iPSC-induced cortical neurons. Further studies will be needed to determine whether these new iPSC-induced model, performing long-lasting experiments, will develop hallmarks of Tau pathology, including Tau hyperphosphorylation, detergent insolubility, Tau mislocalisation and formation of aggregates. This new model will also allow to study if a moderate Tau accumulation may cause disease-relevant cellular phenotypes, such as synaptic dysfunction, neuronal loss, alteration of neuronal morphology (neuritic varicosity, torturous processes). To conclude, we believe that these iPSC-derived models could be a pertinent tool to investigate the pathophysiological mechanisms of Tau-mediated neurodegeneration in the 17q21.31 duplication context, and importantly, to elucidate how a same genetic cause could lead to distinct types of tauopathies.

CRediT authorship contribution statement

Laetitia Miguel: Conceptualization, Methodology, Investigation, Visualization, Writing – review & editing. **Anne Rovelet-Lecrux:** Conceptualization, Investigation, Writing – review & editing. **Pascal Chambon:** Investigation, Resources. **Géraldine Joly-Helas:** Investigation, Resources. **Stéphane Rousseau:** Investigation. **David Wallon:**

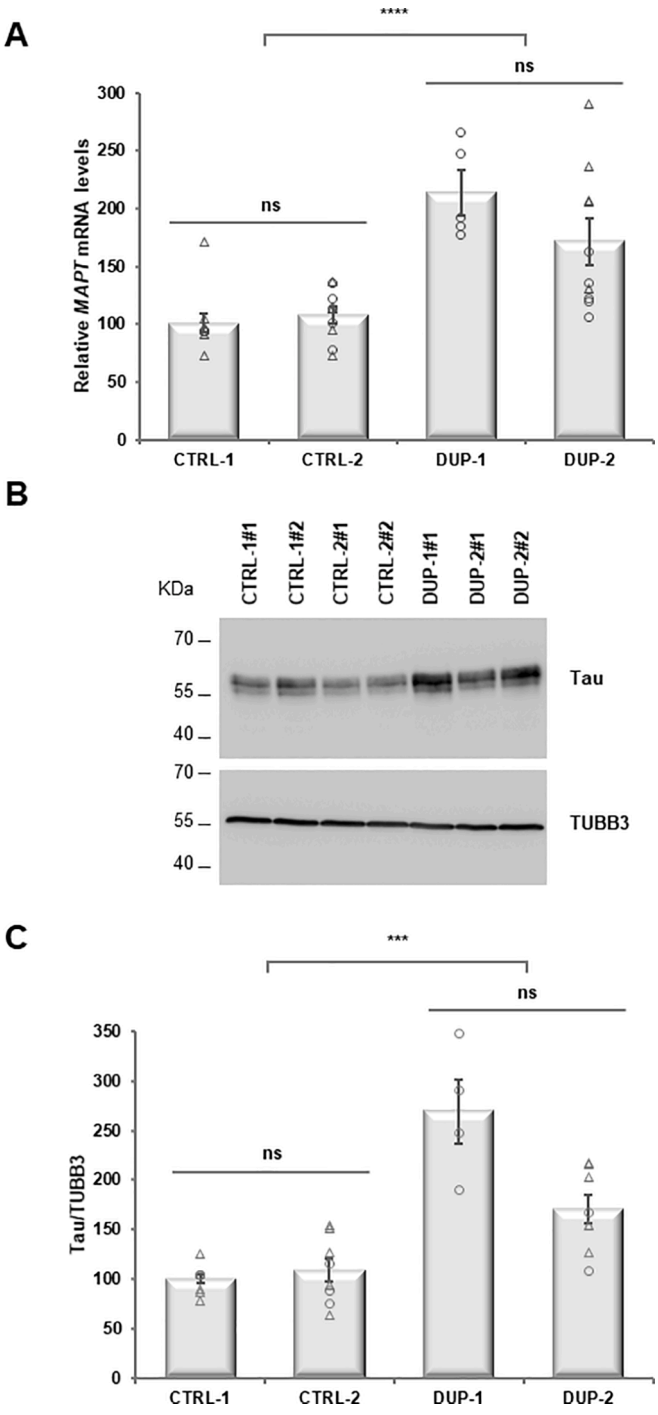

Fig. 4. 17q21.31 duplication causes an increase in Tau both at the mRNA and protein level in iPSC-induced neurons. (A) *MAPT* mRNA quantification by RT-qPCR of mRNA extracted from 3-weeks differentiated iPSC-induced neurons derived from patients and controls using *MAP2* as housekeeping gene. For each clone, 5 biological replicates have been assessed. Clones from the same individual have been pooled. CTRL-1 was arbitrarily set at 100 arbitrary units. CTRL-1 and CTRL-2 expressed similar levels of *MAPT* mRNA (Student's *t*-test, $p = 0.4452$). Although DUP-1 accumulated more *MAPT* mRNA than DUP-2, this trend was not significant (Student's *t*-test, $p = 0.1359$). Importantly, the DUP group accumulated significantly more *MAPT* mRNA than the control group (Student's *t*-test, $p < 0.0001$). (B) Western blot analysis of proteins extracted from iPSC-induced neurons derived from patients and controls using a total Tau antibody. TUBB3 staining was used as a loading control. Tau proteins migrated between 50 and 60 kDa as several bands likely corresponding to different phosphorylation states in control cells. Tau migration profile was similar in patient's cells. Representative blots are presented. (C) Quantification of Tau and TUBB3 signals. CTRL-1 was arbitrarily set at 100 arbitrary units. For each clone, 4 biological replicates have been assessed. Clones from the same individual have been pooled. CTRL-1 and CTRL-2 accumulated similar levels of Tau proteins (Student's *t*-test, $p = 0.5106$). Even if DUP-1 was accumulating more Tau proteins than DUP-2, this trend did not reach statistical significance (Student's *t*-test, $p = 0.0698$). The patients' (DUP) group accumulated significantly more Tau proteins than the CTRL group (Student's *t*-test, $p = 0.0004$). (A) and (C) Circles and triangles correspond to clones 1 and 2, respectively.

Resources, Writing – review & editing. **Stéphane Epelbaum:** Resources, Writing – review & editing. **Thierry Frébourg:** Funding acquisition. **Dominique Campion:** Funding acquisition. **Gaël Nicolas:** Writing – review & editing, Funding acquisition. **Magalie Lecourtois:** Conceptualization, Supervision, Writing – review & editing.

Declaration of Competing Interest

The authors declare that they have no known competing financial interests or personal relationships that could have appeared to influence the work reported in this paper.

Acknowledgements

We would like to thank the Laboratory of Cytogenetics of Rouen University Hospital, France for their help in fibroblast primary culture establishment and karyotype analyses, the iPSC Core facility of Nantes for the fibroblasts reprogramming and helpful technical advices and Sebastien Feuillette for his technical help in the imaging of iPSC-induced neurons. This work was supported by the Fondation pour la Recherche Médicale (Equipe FRM DEQ20170336711).

Appendix A. Supplementary data

Supplementary data to this article can be found online at https://doi.org/10.1016/j.scr.2022.102762.

References

Beevers, J.E., Lai, M.C., Collins, E., Booth, H.D.E., Zambon, F., Parkkinen, L., Vowles, J., Cowley, S.A., Wade-Martins, R., Caffrey, T.M., 2017. MAPT genetic variation and neuronal maturity alter isoform expression affecting axonal transport in iPSC-derived dopamine neurons. Stem Cell Rep. 9, 587–599. https://doi.org/10.1016/j.stemcr.2017.06.005.

Caillet-Boudin, M.-L., Buée, L., Sergeant, N., Lefebvre, B., 2015. Regulation of human MAPT gene expression. Mol. Neurodegener. 10, 28. https://doi.org/10.1186/s13024-015-0025-8.

Chen, Z., Chen, J.A., Shatunov, A., Jones, A.R., Kravitz, S.N., Huang, A.Y., Lawrence, L., Lowe, J.K., Lewis, C.M., Payan, C.A.M., Lieb, W., Franke, A., Deloukas, P., Amouyel, P., Tzourio, C., Dartigues, J.-F., Ludolph, A., Bensimon, G., Leigh, P.N., Bronstein, J.M., Coppola, G., Geschwind, D.H., Al-Chalabi, A., 2019. Genome-wide survey of copy number variants finds MAPT duplications in progressive supranuclear palsy. Mov. Disord. Off. J. Mov. Disord. Soc. 34, 1049–1059. https://doi.org/10.1002/mds.27702.

Ferrer, I., López-González, I., Carmona, M., Arregui, L., Dalfó, E., Torrejón-Escribano, B., Diehl, R., Kovacs, G.G., 2014. Glial and neuronal tau pathology in tauopathies: characterization of disease-specific phenotypes and tau pathology progression. J. Neuropathol. Exp. Neurol. 73, 81–97. https://doi.org/10.1097/NEN.0000000000000030.

García-León, J.A., Cabrera-Socorro, A., Eggermont, K., Swijsen, A., Terryn, J., Fazal, R., Nami, F., Ordovás, L., Quiles, A., Lluis, F., Serneels, L., Wierda, K., Sierksma, A., Kreir, M., Pestana, F., Van Damme, P., De Strooper, B., Thorrez, L., Ebneth, A., Verfaillie, C.M., 2018. Generation of a human induced pluripotent stem cell-based model for tauopathies combining three microtubule-associated protein TAU mutations which displays several phenotypes linked to neurodegeneration. Alzheimers Dement. J. Alzheimers Assoc. 14, 1261–1280. https://doi.org/10.1016/j.jalz.2018.05.007.

Goedert, M., Jakes, R., Vanmechelen, E., 1995. Monoclonal antibody AT8 recognises tau protein phosphorylated at both serine 202 and threonine 205. Neurosci. Lett. 189, 167–169. https://doi.org/10.1016/0304-3940(95)11484-e.

Goedert, M., Spillantini, M.G., Potier, M.C., Ulrich, J., Crowther, R.A., 1989. Cloning and sequencing of the cDNA encoding an isoform of microtubule-associated protein tau containing four tandem repeats: differential expression of tau protein mRNAs in human brain. EMBO J. 8, 393–399.

Greenberg, S.G., Davies, P., Schein, J.D., Binder, L.I., 1992. Hydrofluoric acid-treated tau PHF proteins display the same biochemical properties as normal tau. J. Biol. Chem. 267, 564–569.

Himmler, A., Drechsel, D., Kirschner, M.W., Martin, D.W., 1989. Tau consists of a set of proteins with repeated C-terminal microtubule-binding domains and variable N-terminal domains. Mol. Cell. Biol. 9, 1381–1388. https://doi.org/10.1128/mcb.9.4.1381-1388.1989.

Hooli, B.V., Kovacs-Vajna, Z.M., Mullin, K., Blumenthal, M.A., Mattheisen, M., Zhang, C., Lange, C., Mohapatra, G., Bertram, L., Tanzi, R.E., 2014. Rare autosomal copy number variations in early-onset familial Alzheimer's disease. Mol. Psychiatry 19, 676–681. https://doi.org/10.1038/mp.2013.77.

Irwin, D.J., 2016. Tauopathies as clinicopathological entities. Parkinsonism Relat. Disord. 22 (Suppl 1), S29–33. https://doi.org/10.1016/j.parkreldis.2015.09.020.

Jicha, G.A., Bowser, R., Kazam, I.G., Davies, P., 1997. Alz-50 and MC-1, a new monoclonal antibody raised to paired helical filaments, recognize conformational epitopes on recombinant tau. J. Neurosci. Res. 48, 128–132. https://doi.org/10.1002/(sici)1097-4547(19970415)48:2<128::aid-jnr5>3.0.co;2-e.

Kent, S.A., Spires-Jones, T.L., Durrant, C.S., 2020. The physiological roles of tau and Aβ: implications for Alzheimer's disease pathology and therapeutics. Acta Neuropathol. (Berl.) 140, 417–447. https://doi.org/10.1007/s00401-020-02196-w.

Kovacs, G.G., 2017. Tauopathies. Handb. Clin. Neurol. 145, 355–368. https://doi.org/10.1016/B978-0-12-802395-2.00025-0.

Le Guennec, K., Quenez, O., Nicolas, G., Wallon, D., Rousseau, S., Richard, A.-C., Alexander, J., Paschou, P., Charbonnier, C., Bellenguez, C., Grenier-Boley, B., Lechner, D., Bihoreau, M.-T., Olaso, R., Boland, A., Meyer, V., Deleuze, J.-F., Amouyel, P., Munter, H.M., Bourque, G., Lathrop, M., Frebourg, T., Redon, R., Letenneur, L., Dartigues, J.-F., Martinaud, O., Kalev, O., Mehrabian, S., Traykov, L., Ströbel, T., Le Ber, I., Caroppo, P., Epelbaum, S., Jonveaux, T., Pasquier, F., Rollin-Sillaire, A., Génin, E., Guyant-Maréchal, L., Kovacs, G.G., Lambert, J.-C., Hannequin, D., Campion, D., Rovelet-Lecrux, A., 2017. 17q21.31 duplication causes prominent tau-related dementia with increased MAPT expression. Mol. Psychiatry 22, 1119–1125. https://doi.org/10.1038/mp.2016.226.

Mailliot, C., Sergeant, N., Bussière, T., Caillet-Boudin, M.L., Delacourte, A., Buée, L., 1998. Phosphorylation of specific sets of tau isoforms reflects different neurofibrillary degeneration processes. FEBS Lett. 433, 201–204. https://doi.org/10.1016/s0014-5793(98)00910-7.

Manuel, M.N., Mi, D., Mason, J.O., Price, D.J., 2015. Regulation of cerebral cortical neurogenesis by the Pax6 transcription factor. Front. Cell. Neurosci. 9, 70. https://doi.org/10.3389/fncel.2015.00070.

Miguel, L., Rovelet-Lecrux, A., Feyeux, M., Frebourg, T., Nassoy, P., Campion, D., Lecourtois, M., 2019. Detection of all adult Tau isoforms in a 3D culture model of iPSC-derived neurons. Stem Cell Res. 40, 101541 https://doi.org/10.1016/j.scr.2019.101541.

Rovelet-Lecrux, A., Hannequin, D., Guillin, O., Legallic, S., Jurici, S., Wallon, D., Frebourg, T., Campion, D., 2010. Frontotemporal dementia phenotype associated with MAPT gene duplication. J. Alzheimers Dis. JAD 21, 897–902. https://doi.org/10.3233/JAD-2010-100441.

Sergeant, N., Wattez, A., Delacourte, A., 1999. Neurofibrillary degeneration in progressive supranuclear palsy and corticobasal degeneration: tau pathologies with exclusively "exon 10" isoforms. J. Neurochem. 72, 1243–1249. https://doi.org/10.1046/j.1471-4159.1999.0721243.x.

Shi, Y., Kirwan, P., Livesey, F.J., 2012. Directed differentiation of human pluripotent stem cells to cerebral cortex neurons and neural networks. Nat. Protoc. 7, 1836–1846. https://doi.org/10.1038/nprot.2012.116.

Verheyen, A., Diels, A., Reumers, J., Van Hoorde, K., Van den Wyngaert, I., van Outryve d'Ydewalle, C., De Bondt, A., Kuijlaars, J., De Muynck, L., De Hoogt, R., Bretteville, A., Jaensch, S., Buist, A., Cabrera-Socorro, A., Wray, S., Ebneth, A., Roevens, P., Royaux, I., Peeters, P.J., 2018. Genetically engineered iPSC-derived FTDP-17 MAPT neurons display mutation-specific neurodegenerative and neurodevelopmental phenotypes. Stem Cell Rep. 11, 363–379. https://doi.org/10.1016/j.stemcr.2018.06.022.

Volpato, V., Webber, C., 2020. Addressing variability in iPSC-derived models of human disease: guidelines to promote reproducibility. Dis. Model. Mech. 13 https://doi.org/10.1242/dmm.042317.

Wallon, D., Boluda, S., Rovelet-Lecrux, A., Thierry, M., Lagarde, J., Miguel, L., Lecourtois, M., Bonnevalle, A., Sarazin, M., Bottlaender, M., Mula, M., Marty, S., Nakamura, N., Schramm, C., Sellal, F., Jonveaux, T., Heitz, C., Le Ber, I., Epelbaum, S., Magnin, E., Zarea, A., Rousseau, S., Quenez, O., Hannequin, D., Clavaguera, F., Campion, D., Duyckaerts, C., Nicolas, G., 2021. Clinical and neuropathological diversity of tauopathy in MAPT duplication carriers. Acta Neuropathol. https://doi.org/10.1007/s00401-021-02320-4.

Wang, Y., Mandelkow, E., 2016. Tau in physiology and pathology. Nat. Rev. Neurosci. 17, 5–21. https://doi.org/10.1038/nrn.2015.1.

Wilson, P.G., Stice, S.S., 2006. Development and differentiation of neural rosettes derived from human embryonic stem cells. Stem Cell Rev. 2, 67–77. https://doi.org/10.1007/s12015-006-0011-1.